Flame Topology and Combustion Instability Limits of Lean Premixed Hydrogen Enriched Flames

I. Chterev, I. Boxx
Institut für Verbrennungstechnik, Deutsches Zentrum für Luft-und Raumfahrt (DLR)

Stuttgart, Germany

Abstract

The operation of a technically premixed, swirl stabilized atmospheric laboratory burner based on the PRECCINSTA with high hydrogen fuel mixtures is demonstrated at various operating conditions across different thermal powers, equivalence ratios and H_2/CH_4 volume fractions up to 50%. The stable and unstable operating conditions are experimentally determined in terms of equivalence ratio and thermal power, and the peak frequencies and amplitudes of thermoacoustically excited cases are measured. This work finds (as expected) that hydrogen addition significantly affects the flame shape and combustion instability limits. Specifically, the flame is made more compact and the flame is observed to change from M to V-shaped at fuel lean conditions, both of which impact combustor thermal loading. Furthermore, hydrogen addition raises the peak frequencies by 5-25%, and modifies the thermoacoustic amplitude.

1 Introduction

Combustion of hydrogen is increasingly relevant to industry as a means of chemical energy storage via hydrolysis from renewable power sources such as solar and wind, and as a means to reduce carbon emissions by power generation. One strategy of implementing hydrogen fuel in industrial gas turbines is displacing some of the natural gas with hydrogen. The different chemical properties of hydrogen present significant combustor design challenges. Namely, the higher flame speed and higher flame temperature of hydrogen imply that the flame will stabilize differently, have a different size and or shape, and exhibit different dynamics. These different combustion physics affect combustor performance parameters such as hardware heat loading, combustor exit pattern factor, ignition and blow-off, and emissions.

Premixed hydrogen-enriched combustion flame stability and emissions have been studied extensively with laboratory model combustors [1-4]. Researchers observed that hydrogen addition lowers the fuel/air equivalence ratio for extinction, changes the extinction dynamics, and can change the flame mode in flow fields with multiple flame stabilization locations. Thermoacoustic oscillations in combustors or combustion instabilities occur when a combustor acoustic mode couples to the heat release via a positive feedback loop. High amplitudes of these oscillations can cause immediate damage or shorten hardware life through increased heat transfer and pressure fluctuations, and are therefore highly undesirable. Hydrogen addition is also observed to change the combustion instability limits and dynamics.

Correspondence to: ianko.chterev@dlr.de

The burner used in this study is based on the PRECCINSTA design, which has been studied widely experimentally [5,6] and computationally [7,8]. The flame shape and combustion instability characteristics are studied using time-resolved (10 kHz) OH* chemiluminescence imaging and two-microphone acoustic measurements.

The objective of this work is two-fold. First, we demonstrate the reliable operation of the technically premixed swirl burner over a range of thermal powers and equivalence ratios with Hydrogen enrichment levels of up to 50% (by volume). Second, we detail the combustion stability characteristics in terms of operating conditions for stable and unstable combustion and the frequencies and amplitudes of the thermoacoustically excited cases.

2 Experiment

Experimental studies were performed at atmospheric pressure in the technically premixed gas turbine model combustor shown in Figure 1 (PRECCINSTA, see refs. 5-8). The air first enters the plenum and then passes through a swirl generator with 12 radial vanes. The fuel is injected through 1mm orifices in the swirl vanes. The swirling flow then enters a combustion chamber through a burner nozzle with an exit diameter of D = 27.85 mm and a conical inner bluff body. The chamber has a square cross-section of 85 × 85 mm^2 and a height of 114 mm. Optical access to the chamber is provided by side walls made of quartz glass held by metal posts in the corners. The exit is composed of a conical part followed by an exhaust duct with 40 mm inner diameter.

Line-of-sight OH* chemiluminescence is a commonly used indicator of heat-release. OH* chemiluminescence signal was collected with an intensified high-speed CMOS camera (LaVision HSS 5 with LaVision HS-IRO) equipped with a fast UV lens (Cerco, f = 45 mm, f/1.8) and a bandpass filter (300–325 nm). The intensifier gate time was between 20 and 50 μs depending on signal strength.

Pressure signals from the combustion chamber were recorded to provide information about combustion dynamics. The pressure in the chamber was measured using amplitude and phase calibrated microphone probes equipped with B&K Type 4939 condenser microphones. One probe was placed in the plenum, and another one in the combustion chamber at a height of x = 20 mm. The signals were recorded simultaneously using a multichannel A/D converter with a sampling rate of 100 kHz.

The background corrected chemiluminescence images were divided by a white field image (also background corrected), produced using a white screen, to compensate for the intensifier and lens non-uniform spatial response. The images were then averaged to produce the flame brush images shown. The acoustic pressure signals were calibrated using the phase and amplitude curve for each probe in frequency space.

Data were collected at various values of thermal power, P_{th} [10, 20, 30 kW], fuel/air equivalence ratio, ϕ [0.70, 0.85, 1.05], and H_2/CH_4 volume fraction [0 to 40% in 5% increments]. The operating conditions are listed in Table 1.

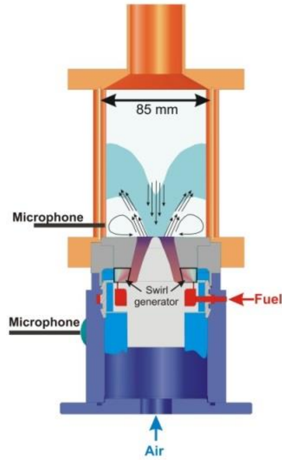

Figure 1: PRECCINSTA premixed swirl burner [5-8]. The shape of the flame zone is indicated in the combustion chamber and the overall flow field is sketched.

Table 1: Operating conditions for the OH* chemiluminescence and acoustic measurements. In some cases 50% H_2 volume fraction could not be reached due to strong thermoacoustics breaking the windows.

Set #	$\dot{Q}$ **[kW]**	**φ**	**% Vol. H_2 (5% incr.)**
1	11	0.70	0-50
2	11	0.85	0-50
3	11	1.05	0-50
4	23	0.70	0-35
5	23	0.85	0-50
6	21	1.05	0-50
7	34	0.70	0-20
8	34	0.85	0-40
9	32	1.06	0-40

3 Results and Discussion

The flame shapes and combustion instability limits with 100% CH_4 are compared to previous measurements [6]. Consistent with prior studies [5-8], two flame shapes are observed: a V-shaped flame at lower values of P_{th} and higher values of ϕ, and an M-shaped flame at higher values of P_{th} and lower ϕ.

Data at the various conditions studied – P_{th} [10, 20, 30 kW], ϕ [0.70, 0.85, 1.05], and H_2/CH_4 volume fraction [0 to 40% in 5% increments] – are shown in Figure 2, Figure 3, and Figure 4. Parts (a) of the figures show the time-averaged flame images. The first columns of parts (a) of the three figures illustrate the baseline fuel behavior [6], i.e. a V-shaped flame is observed at lower values of P_{th} and higher values of ϕ, and an M-shaped flame at higher values of P_{th} and lower ϕ.

Parts (b) show the associated acoustic pressure values, p_{RMS}, and peak frequencies, f_n. The peak frequencies were determined via the application of a fast Fourier transform (FFT) to the acoustic pressure measurement. Figure 5 shows a sample frequency spectra acquired in a flame at ϕ=0.85 and 10 kW. In this case there are actually two peak frequencies, with the higher one having a higher amplitude. The relative peak strength is here represented by the Signal-to-Background Ratio (SBR), calculated as the ratio of the amplitude of interest to the average background amplitude. Narrow peaks result in higher amplitudes, and hence, higher values of SBR. In interpreting the figures to determine whether or not the burner is unstable we look for a simultaneous discontinuous change in the p_{RMS} and SBR.

Still considering the 0% hydrogen case, at 10 kW (Figure 2(b), first column), there are no simultaneous discontinuous changes in the p_{RMS} and SBR, but for the 20 kW case with 0% hydrogen (Figure 3(b), column 1) we observe a marked rise in the p_{RMS} from 53 to 98 Pa with a corresponding rise in the SBR from 3 to 16 as ϕ is dropped from 1.05 to 0.85. For the 20 kW case as ϕ is dropped further to 0.70, the peak amplitude (300 Pa) and SBR (15) remain high. For the 30 kW case with 0% hydrogen (Figure 4(b) column 1) again no accompanying discontinuous changes in p_{RMS} and SBR are observed.

Next, considering the effect of hydrogen addition from 0 to 20% to 40% on flame shape (columns 1, 2 and 3 in Figure 2 through Figure 4, parts (a)) it is apparent that hydrogen addition results in a transition from an M- or M-like flame to a V-flame, for all three powers at the leanest ϕ=0.70, but more notably for the higher, 20 and 30kW cases. Parts (b) of the same figures indicate that hydrogen addition can either:

(1) activate a thermoacoustic instability (all 10 kW cases, ϕ=0.70 and 0.85 cases at 30 kW);

(2) modify the amplitudes of already active thermoacoustics (i.e. ϕ =0.70 at 20 kW);

(3) deactivate a thermoacoustic instability (i.e. ϕ =0.85 at 20 kW); and

(4) have minimal effects on the thermoacoustics stability (ϕ =1.05 at 20 and 30 kW).

For all cases, hydrogen addition is observed to shorten the flame and causes it to stabilize closer to the combustor nozzle exist plane, suggesting increased thermal loading to the combustor hardware. Hydrogen addition also consistently raises the peak frequencies by about 5-25%. This is likely as a result of changes to the product fluid dynamic properties and flame response. As mentioned before a detailed discussion of the thermoacoustic mechanism and how the thermoacoustic frequencies are determined is deferred to a later paper.

As mentioned, the thermoacoustic amplitudes are modified. Whether the amplitude goes up or down depends on the balance between the change to the driving frequency, and therefore combustor acoustic response, and the feedback loop strength. The former can be illustrated as follows: if the driving frequency is shifted closer to a resonant peak of the combustor where the response is higher, the response amplitude is expected to increase; conversely if the driving frequency is shifted away from a resonant peak, the response amplitude is expected to decrease. The feedback loop strength depends on the detailed interactions between the acoustic field and heat release, and is also outside of the scope of this work.

Sometimes a single dominant peak frequency is observed, and sometimes one or more additional higher frequencies usually with lower amplitudes but sometimes higher are observed. The single-mode cases are marked in red, while the multi-mode cases are marked in yellow in Figure 2 through Figure 4.

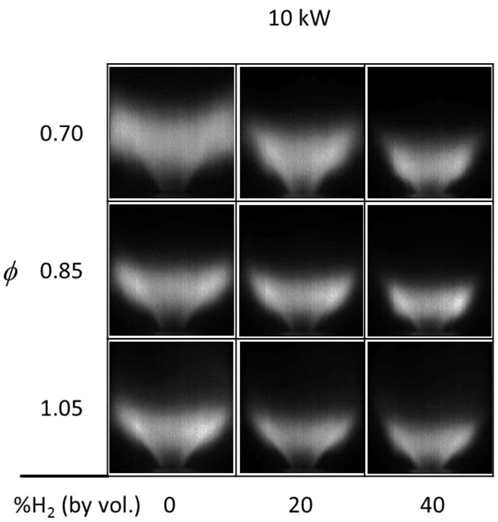

p_{RMS} [Pa]
Nth Peak Frequency:
f_n [Hz] (SBR)

ϕ \ %H$_2$	0	20	40
0.70	p_{RMS}=48.9 f_1=202 (13)	p_{RMS}=125 f_1=248 (26) f_2=495 (4.5)	p_{RMS}=130 f_1=261 (25) f_2=523 (4.7)
0.85	p_{RMS}=33.7 f_1=227 (4.3) f_2=532 (3.2)	p_{RMS}=39.4 f_1=249 (6.3)	p_{RMS}=105 f_1=273 (13.1) f_2=467 (18.3)
1.05	p_{RMS}=19.1 f_1=240 (5.6)	p_{RMS}=22.9 f_1=246 (6.7)	p_{RMS}=54.0 f_1=255 (25) f_2=510 (6.2)

Figure 2: 10 kW thermal power (P_{th}): (a) Flame shapes as ϕ vs. H_2/CH_4 by volume; (b) Sound pressure level (p_{RMS}), and peak frequencies and Signal-to-Background Ratio (SBR).

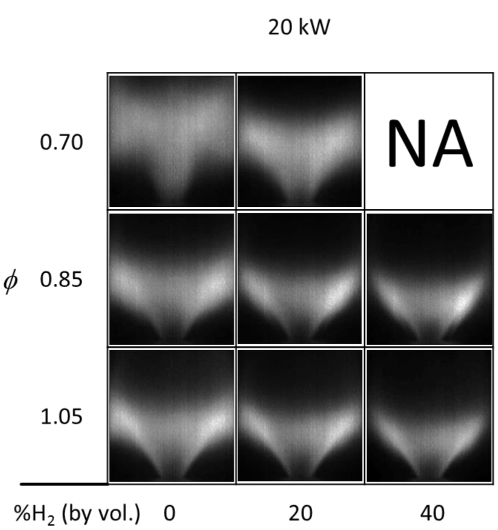

p_{RMS} [Pa]
Nth Peak Frequency:
f_n [Hz] (SBR)

ϕ \ %H$_2$	0	20	40
0.70	p_{RMS}=300 f_1=262 (15) f_2=529 (5.5)	p_{RMS}=437 f_1=322 (40) f_2=640 (11)	NA
0.85	p_{RMS}=97.7 f_1=292 (16)	p_{RMS}=65.4 f_1=323 (7.4)	p_{RMS}=62.9 f_1=375 (3.9)
1.05	p_{RMS}=53.4 f_1=344 (2.7)	p_{RMS}=50.3 f_1=400 (4.4)	p_{RMS}=52.3 f_1=410 (3.7)

Figure 3: 20 kW thermal power (P_{th}): (a) Flame shapes as ϕ vs. H_2/CH_4 by volume; (b) Sound pressure level (p_{RMS}), and peak frequencies and Signal-to-Background Ratio (SBR).

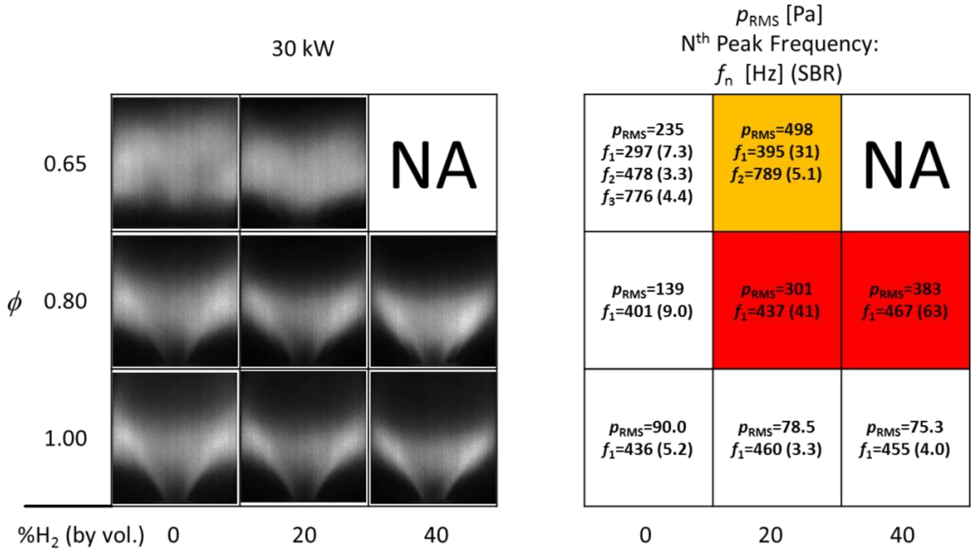

Figure 4: 30 kW thermal power (P_{th}): (a) Flame shapes as ϕ vs. H_2/CH_4 by volume; (b) Sound pressure level (p_{RMS}), and peak frequencies and Signal-to-Background Ratio (SBR).

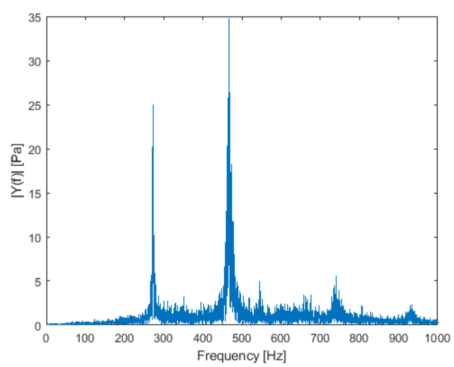

Figure 5: Sample FFT plot for ϕ =0.85 at 10 kW. p_{RMS}=110 Pa.

4 Concluding Remarks

The flame shape and combustion stability characteristics of lean, swirl-stabilized flames of hydrogen-enriched methane in a technically premixed gas turbine model combustor (PRECCINSTA) operated at atmospheric pressure were studied using time-resolved (10 kHz) OH* chemiluminescence imaging and acoustic pressure measurements. Fuel/air equivalence ratio and thermal power were varied, as well as the H_2/CH_4 volume fraction up to 40%. The stability characteristics are experimentally described in terms of operating conditions (Pth, and equivalence ratio) for stable/unstable operation, and the frequencies and amplitude of the thermoacoustic fluctuations for unstable operation. Across all operating conditions, hydrogen addition is observed to:

(1a) shorten the flame, likely due to faster combustion chemistry, i.e. flame speed;

(1b) cause the flame to stabilize closer to the combustor nozzle exit plane, again, likely due to its effect on flame speed;

(2) modify the thermoacoustic fluctuation amplitude and number of active modes; and

(3) raise the peak thermoacoustic frequencies.

The observed effects have engineering implications on the design of gas combustors for the operation with high hydrogen enrichment. The shortened flames and their shift closer to the combustor nozzle would likely increase the hardware peak temperatures and hardware stress, requiring consideration and possible design changes. Understanding the combustor thermoacoustic stability boundaries is also important for the design of reliable hardware.

References

[1] Lieuwen T, McDonell V, Santavicca D, Sattelmayer T. (2008). Burner development and operability issues associated with steady flowing syngas fired combustors. Combust. Sci. Technol., 180(6): 1169.

[2] Shanbhogue SJ, Sanusi YS, Taamallah S, Habib MA, Mokheimer EMA, Ghoniem AF. (2016). Flame macrostructures, combustion instability and extinction strain scaling in swirl-stabilized premixed CH4/H2 combustion. Combust. Flame. 163: 494.

[3] Ghoniem AF, Annaswamy A, Park S, Sobhani ZC. (2005). Stability and emissions control using air injection and H2 addition in premixed combustion. Proc. Combust. Inst. 30(2): 1765.

[4] Zhang Q, Noble DR, Lieuwen T. (2007). Characterization of Fuel Composition Effects in H2/CO/CH4 Mixtures Upon Lean Blowout. J. Eng. Gas Turb. Power. 129(3): 688.

[5] Meier W, Weigand P, Duan XR, Giezendanner-Thoben R. (2007). Detailed characterization of the dynamics of thermoacoustic pulsations in a lean premixed swirl flame. Combust. Flame. 150(1-2): 2.

[6] Oberleithner K, Stöhr M, Im SH, Arndt CM, Steinberg AM. (2015). Formation and flame-induced suppression of the precessing vortex core in a swirl combustor: experiments and linear stability analysis. Combust. Flame. 162(8): 3100.

[7] Fiorina B, Vicquelin R, Auzillon P, Darabiha N, Gicquel O, Veynante D. (2010). A filtered tabulated chemistry model for LES of premixed combustion. Combust. Flame. 157(3): 465.

[8] Wang P, Platova NA, Fröhlich J, Maas U. (2014). Large eddy simulation of the PRECCINSTA burner. Int. J. Heat Mass Transfer. 70: 486.